

## RESEARCH ARTICLE

# Comparative interactomics analysis reveals potential regulators of $\alpha6\beta4$ distribution in keratinocytes

Lisa te Molder<sup>1</sup>, Liesbeth Hoekman<sup>2</sup>, Maaïke Kreft<sup>1</sup>, Onno Bleijerveld<sup>2</sup> and Arnoud Sonnenberg<sup>1,\*</sup>

## ABSTRACT

The integrin  $\alpha6\beta4$  and cytoskeletal adaptor plectin are essential components of type I and type II hemidesmosomes (HDs). We recently identified an alternative type II HD adhesion complex that also contains CD151 and the integrin  $\alpha3\beta1$ . Here, we have taken a BioID proximity labeling approach to define the proximity protein environment for  $\alpha6\beta4$  in keratinocytes. We identified 37 proteins that interacted with both  $\alpha6$  and  $\beta4$ , while 20 and 78 proteins specifically interacted with the  $\alpha6$  and  $\beta4$  subunits, respectively. Many of the proximity interactors of  $\alpha6\beta4$  are components of focal adhesions (FAs) and the cortical microtubule stabilizing complex (CMSC). Though the close association of CMSCs with  $\alpha6\beta4$  in HDs was confirmed by immunofluorescence analysis, CMSCs have no role in the assembly of HDs. Analysis of the  $\beta4$  interactome in the presence or absence of CD151 revealed that they are strikingly similar; only 11 different interactors were identified. One of these was the integrin  $\alpha3\beta1$ , which interacted with  $\alpha6\beta4$  more strongly in the presence of CD151 than in its absence. These findings indicate that CD151 does not significantly contribute to the interactome of  $\alpha6\beta4$ , but suggest a role of CD151 in linking  $\alpha3\beta1$  and  $\alpha6\beta4$  together in tetraspanin adhesion structures.

**KEY WORDS:** Integrin, Interactome, BioID, Hemidesmosome, Cortical microtubule stabilizing complex, Tetraspanin

## INTRODUCTION

The cytoskeleton of epithelial cells is an integrated network of actin microfilaments, keratin intermediate filaments and microtubules, which helps the cell to maintain its shape and internal organization. The actin and keratin networks are linked to the cytoskeletons of adjacent cells and the extracellular matrix by specialized junctional complexes and, thereby, contribute to tissue integrity and intracellular communication (Kirfel et al., 2003; Blanchoin et al., 2014). While the microtubule cytoskeleton is responsible for the intracellular transport of membrane-bound vesicles and organelles.

Hemidesmosomes (HDs) are integrin-based adhesion complexes that mediate stable anchorage of epithelial cells to the underlying basement membrane and serve as anchoring sites for the keratin

cytoskeleton to the plasma membrane. Two types of HDs can be distinguished according to their protein composition. The integrin  $\alpha6\beta4$ , a heterodimeric transmembrane protein, is the main component of both type I and type II HDs (Uematsu et al., 1994; Fontao et al., 1997; Sterk et al., 2000; Litjens et al., 2006; Walko et al., 2015). In addition to  $\alpha6\beta4$ , these two structures share the tetraspanin CD151 and the cytoskeletal linker protein plectin, which through binding to  $\beta4$  and keratin establishes a linkage between the extracellular matrix (ECM) and the keratin intermediate filament (IF) cytoskeleton. In type I HDs an additional linkage between the plasma membrane and keratin filaments through BP180 and BP230 enhances the stability of these adhesion structures. A third CD151-containing adhesion structure formed in the central region of cultured keratinocytes contains the integrin  $\alpha3\beta1$  in addition to the type II HD components  $\alpha6\beta4$  and plectin (te Molder et al., 2019). Absence or defects of HD proteins compromises epithelial integrity, which results in a blistering disorder called Epidermolysis Bullosa (Has and Bruckner-Tuderman, 2014). Besides its role in mediating stable cell-matrix adhesion, the HD integrin  $\alpha6\beta4$  cooperates with growth factor receptors to promote pro-tumorigenic signaling (Ramovs et al., 2017).

Linkage of the actin cytoskeleton to the extracellular matrix occurs (amongst others) at integrin-based multiprotein complexes termed focal adhesions (FAs). The molecular composition of these adhesions may vary depending on external cues and cellular responses (Horton et al., 2015). However, their core always consists of integrins and adaptor proteins such as talin and vinculin. In addition to providing adhesion of the cells, FAs are essential for cell migration.

In close proximity of FAs, cytoplasmic linker associated proteins (CLASPs) anchor the plus ends of microtubules to the plasma membrane through a complex of LL5 $\alpha/\beta$  (also known as PHLDB1/2), liprin  $\alpha1/\beta1$  and ELKs (also known as ERC1) (Mimori-Kiyosue et al., 2005; Lansbergen et al., 2006; Akhmanova and Steinmetz, 2008). KANK proteins have been identified as the adaptor proteins that can link this complex of proteins, known as the cortical microtubule stabilizing complexes (CMSCs), to FAs. They bind on the one hand to talin in FAs and on the other hand to liprin  $\beta1$  in the CMSCs. By serving as sites for the targeted delivery of microtubule bound vesicles containing MMPs at the cell membrane, the CMSCs are thought to play an important role in the turnover of FAs and actin reorganization (Rodríguez et al., 2003; Akhmanova et al., 2009; Stehbins et al., 2014; Dogterom and Koenderink, 2019).

Recently, we showed that FAs and HDs are mechanically coupled, and that plectin, which binds integrin  $\beta4$  and F-actin in a mutually exclusive manner, plays a central role in this coupling (Wang et al., 2020). In this study, we used proximity dependent biotinylation (BioID) (Roux et al., 2012) to map the interactomes of the integrin  $\alpha6$  and  $\beta4$  subunits in keratinocytes and assessed the contribution of CD151 to the  $\beta4$  interactome. Furthermore, we investigated the role of CMSC components in HD dynamics.

<sup>1</sup>Division of Cell Biology I, The Netherlands Cancer Institute, Plesmanlaan 121, Amsterdam 1066 CX, The Netherlands. <sup>2</sup>Mass Spectrometry/Proteomics Facility, The Netherlands Cancer Institute, Plesmanlaan 121, Amsterdam 1066 CX, The Netherlands.

\*Author for correspondence (a.sonnenberg@nki.nl)

© L.H., 0000-0002-3552-6390; M.K., 0000-0003-1301-2898; O.B., 0000-0002-9395-2347; A.S., 0000-0001-9585-468X

This is an Open Access article distributed under the terms of the Creative Commons Attribution License (<https://creativecommons.org/licenses/by/4.0>), which permits unrestricted use, distribution and reproduction in any medium provided that the original work is properly attributed.

## RESULTS

**Identification of the  $\beta 4$  associated proteins by proximity-dependent biotinylation**

To identify proteins that interact with integrin  $\alpha 6\beta 4$  in keratinocytes, we applied the BioID method (Roux et al., 2012), which has been successfully used to identify proteins that reside in close proximity of a specific protein of interest, including proteins that are only transiently associated (van Itallie et al., 2013, 2014; Fredriksson et al., 2015; Dong et al., 2016). BioID employs a modified biotin ligase BirA\* fused to a protein of interest that biotinylates proteins in close proximity (20 nm) upon addition of biotin. We fused BirA\* to the C-terminal tail of full-length integrin  $\beta 4$  (Fig. 1A) and stably expressed the fusion protein in  $\beta 4$ -deficient PA-JEB keratinocytes by retroviral transduction. Expression of the  $\beta 4$ -BirA\* fusion protein (225 kDa) was confirmed by western blot (Fig. 1B). Like wild-type  $\beta 4$ , the fusion protein localized in HDs as visualized by immunofluorescence (Fig. 1C).

Treatment of the  $\beta 4$ -BirA\* expressing cells with biotin resulted in a time-dependent increase in biotinylated proteins (Fig. 1D). Notably, a number of proteins were biotinylated in the absence of exogenously added biotin. In an effort to reduce the level of biotinylation of these background proteins, we depleted the culture medium of biotin by treatment with Streptavidin agarose beads, which reduced the amount of background proteins (Fig. 1E).

Biotinylated proteins were collected using streptavidin-Sepharose beads and analyzed by mass spectrometry. As expected, the integrin  $\beta 4$  subunit and its partner subunit  $\alpha 6$ , were identified among 130 other hits. Other interactors were components of HDs and multiple proteins of two other membrane complexes, CMSCs and FAs (Fig. 1F; Table S1).

**Interactomics analysis of  $\alpha 6\beta 4$ -associated proteins**

To demonstrate the specificity of the  $\beta 4$  interactions with components of FAs and CMSCs, we performed an additional BioID experiment with an irrelevant transmembrane protein, the interleukin2 receptor

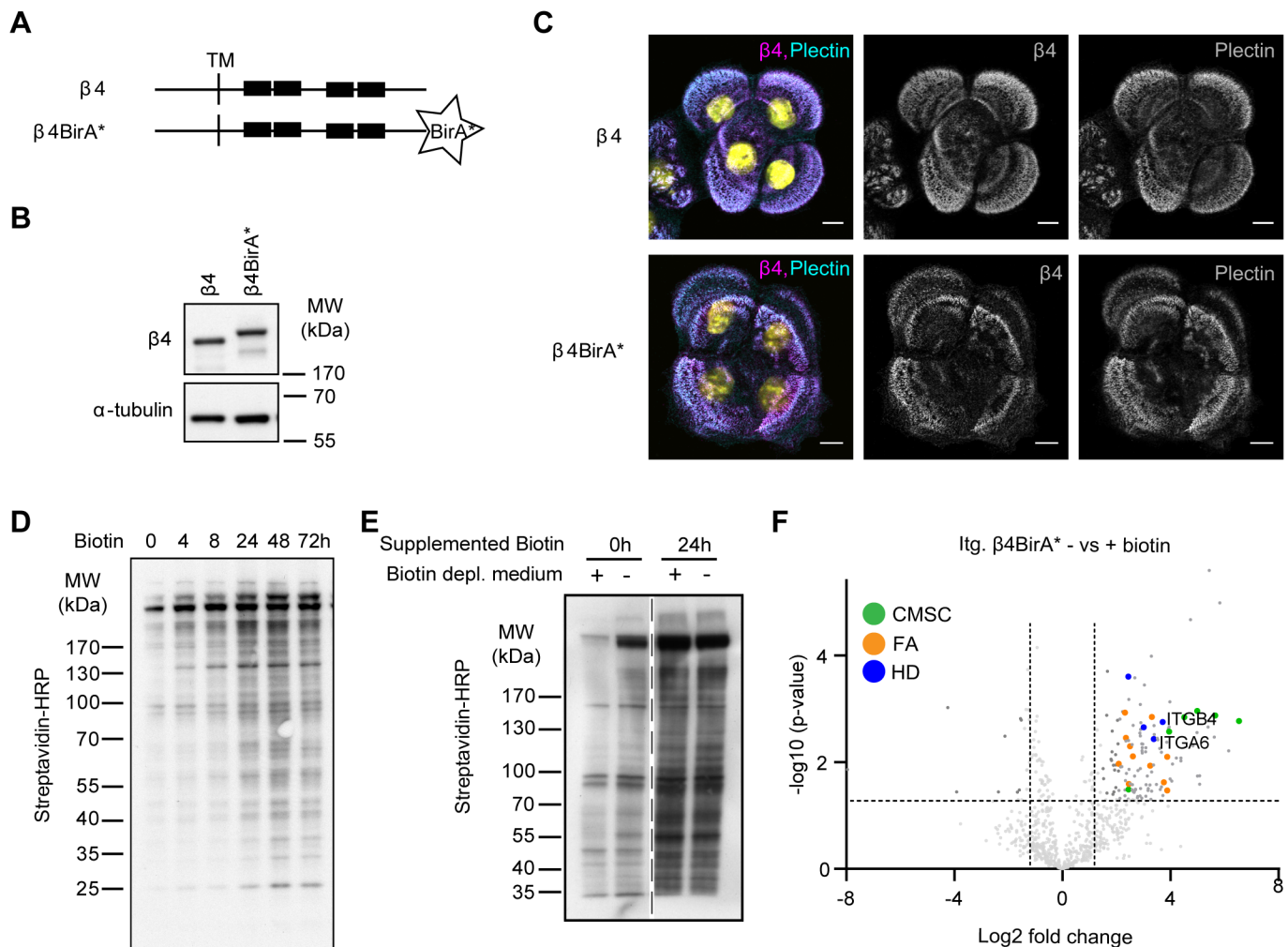


**Fig. 1. BioID method to identify  $\beta 4$  proximity interactors.** (A) Schematic representation of wild-type  $\beta 4$  and the  $\beta 4$ -BirA\* fusion proteins. Black boxes indicate the FnIII domains. TM is transmembrane domain. (B) Western blot analysis of whole cell lysates from PA-JEB/ $\beta 4$  and PA-JEB/ $\beta 4$ -BirA\* keratinocytes probed with anti- $\beta 4$  and anti- $\alpha$ -tubulin (loading control) antibodies. (C) Representative confocal microscopy images of PA-JEB keratinocytes expressing wild-type  $\beta 4$  and  $\beta 4$ -BirA\* stained for  $\beta 4$  and plectin. Scale bars: 10  $\mu$ m. (D) Whole cell lysates from PA-JEB/ $\beta 4$ -BirA\* keratinocytes treated for the indicated time points with 50  $\mu$ M biotin and analyzed by western blot with streptavidin-HRP. (E) Western blot analysis of biotinylated proteins from PA-JEB/ $\beta 4$ -BirA\* cells, cultured in regular medium or biotin-depleted medium for 20 h and subsequently treated with or without biotin for 24 h. Biotinylated proteins were detected by probing the membrane with Streptavidin-HRP. (F) Volcano plot showing enrichment ( $\log_2$ ) and corresponding significance ( $P$ -value,  $\log_{10}$ ) of biotinylated proteins in biotin-treated and -untreated PA-JEB/ $\beta 4$ -BirA\* keratinocytes ( $n=3$ ).

(IL2R). Stable cell lines expressing the IL2R fused to BirA\* were generated by retroviral infection. The IL2R-BirA\* fusion protein was expressed in PA-JEB/ $\beta$ 4 keratinocytes. Pairwise comparison of the  $\beta$ 4-BirA\* and IL2R-BirA\* datasets (obtained after treatment of the cells with 50  $\mu$ M biotin) revealed that 115 proteins interacted specifically with integrin  $\beta$ 4. Consistent with the results of the comparison of the  $\beta$ 4 samples treated with or without biotin, we identified multiple HD proteins (5/6) and FA proteins (10/60), and all components of the CMSC (7/7) as proximity interactors of  $\beta$ 4 (Fig. 2A; Table S2).

Next, we determined the proximity interactors of the integrin  $\alpha$ 6 subunit. To this end, the  $\alpha$ 6 subunit fused to BirA\* was expressed in PA-JEB/ $\beta$ 4 keratinocytes, in which the  $\alpha$ 6 gene (*ITGA6*) had been disrupted by CRISPR/Cas9 technology. Expression and localization of the  $\alpha$ 6-BirA\* fusion protein in HDs was confirmed by western blot and immunofluorescence analyses (Fig. 2B,C).

A total of 57 proximity interactors of  $\alpha$ 6 were identified that were absent from the negative IL2R-BirA\* sample. 37 of these proteins were also identified in the  $\beta$ 4 interactome. Again, many of the shared proteins were components of HDs, CMSCs and FAs (Fig. 2E). The analysis also revealed a significant number of subunit-specific interactors, 20 for  $\alpha$ 6 and 78 for  $\beta$ 4 (Fig. 2D). The fact that more proteins were identified with  $\beta$ 4-BirA\* than with  $\alpha$ 6-BirA\* could be due to flexibility of the unusually long  $\beta$ 4 cytoplasmic domain (1019 amino acids compared to 54 amino acids in  $\alpha$ 6), which allows the fused biotin ligase not only to biotinylate proteins that are spatially located near to but also distant from the  $\alpha$ 6 subunit. It is important to note that keratinocytes do not express  $\alpha$ 6 $\beta$ 1 and that, therefore, the interactors of  $\alpha$ 6 subunit can be considered to be specific for  $\alpha$ 6 $\beta$ 4 (Table S3) (Sonnenberg et al., 1991; te Molder et al., 2019).

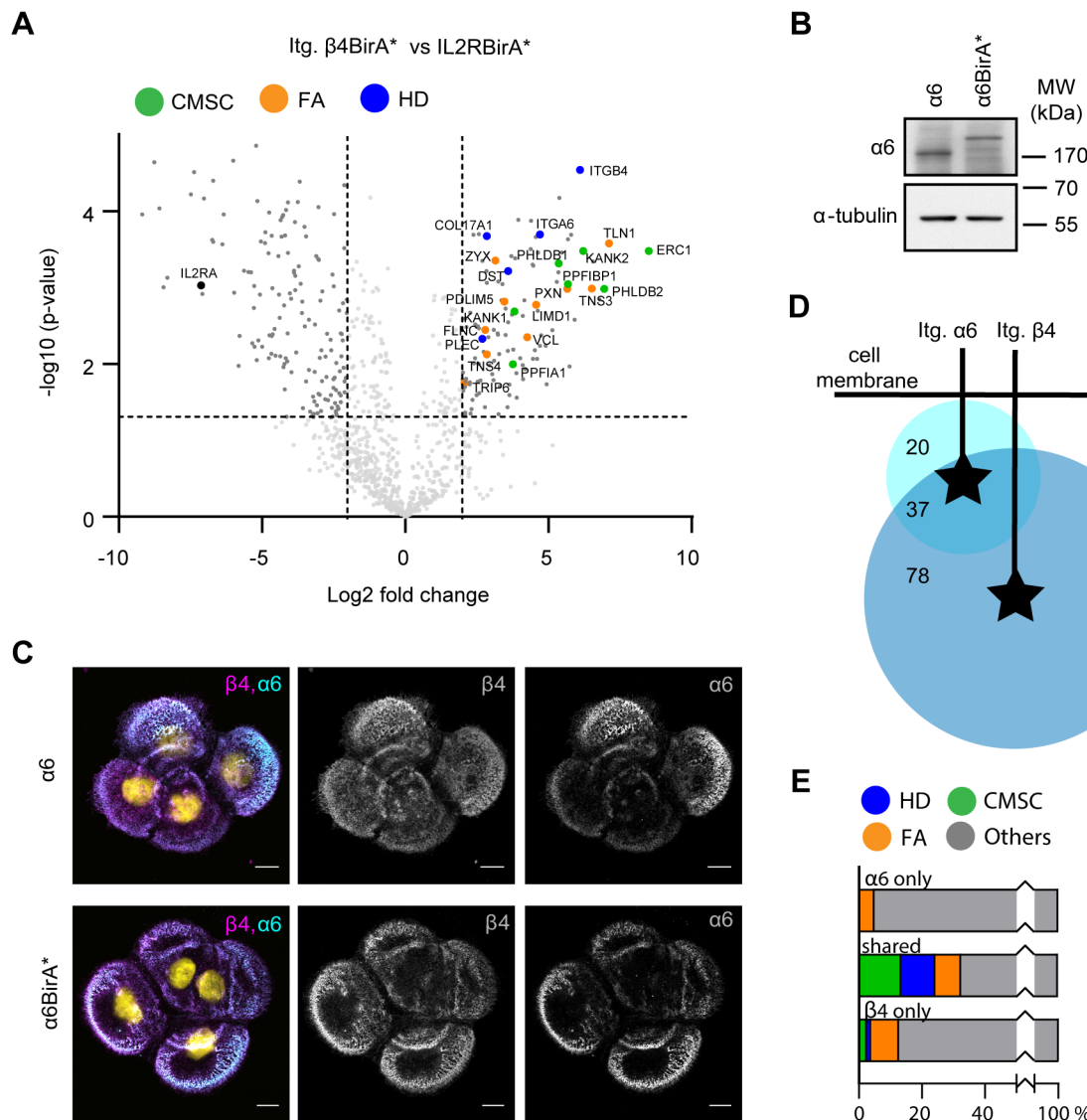


**Fig. 2. Interactomics analysis of  $\alpha$ 6 $\beta$ 4 associated proteins.** (A) Volcano plot showing enrichment ( $\log_2$ ) versus significance ( $P$ -value,  $\log_{10}$ ) of proteins identified by  $\beta$ 4-BirA\* relative to control IL2R-BirA\* ( $n=3$ ). Components of the CSMCs, FAs and HDs are highlighted in green, orange and blue, respectively. (B) Western blot analysis of whole cell lysates from PA-JEB/ $\beta$ 4 and PA-JEB/ $\beta$ 4  $\alpha$ 6-BirA\* keratinocytes probed with anti- $\alpha$ 6 and anti- $\alpha$ -tubulin (loading control) antibodies. (C) Representative confocal microscopy images of PA-JEB/ $\beta$ 4 keratinocytes expressing endogenous  $\alpha$ 6 or  $\alpha$ 6-BirA\* stained for  $\alpha$ 6 and  $\beta$ 4. Scale bars: 10  $\mu$ m. (D) Venn diagram depicting the number of overlapping hits between interacting proteins of the Itg.  $\alpha$ 6 and Itg.  $\beta$ 4 subunit. Numbers of overlapping and specific proteins are presented. (E) Bar graphs showing the percentage of HD, CMSC and FA proteins in the  $\alpha$ 6 and  $\beta$ 4 interactomes as well as their percentage among the interactors shared by the two interactomes.



In conclusion, the interactome of integrin  $\alpha 6\beta 4$  in keratinocytes contains 135 proteins, and many of the previously mentioned HD, CMSC and FA proteins were among the significant interactors of both  $\alpha 6$  and  $\beta 4$ .

### $\beta 4$ proximity interactors in the presence and absence of CD151

Previously, we have shown that  $\alpha 6\beta 4$  resides in both central and peripheral adhesions in keratinocytes (te Molder et al., 2019). While the peripheral adhesions have all the hallmarks of type I HDs, the central adhesions are more similar to type II HDs but are not associated with keratin filaments and, additionally, contain integrin  $\alpha 3\beta 1$ . Because CD151 forms a complex with both  $\alpha 3\beta 1$  and  $\alpha 6\beta 4$ , and plays an important role in promoting the formation of the central HD-like adhesions, we wondered whether some of the components of the  $\beta 4$  interactome depend on the presence of CD151. To this end, we generated CD151-deficient PA-JEB/ $\beta 4$ -BirA\* keratinocytes by CRISPR/Cas9-mediated gene disruption and subjected them to BioID. Deletion of CD151 was confirmed by FACS analysis (Fig. 3A). BioID results showed that the  $\beta 4$  interactomes in CD151-proficient and -deficient keratinocytes overlapped each other almost

completely; only 11 different  $\beta 4$  interactors were identified (Fig. 3B Table S4). Integrin  $\alpha 3\beta 1$ , a CD151 binding partner was significantly more associated with  $\beta 4$  in the presence of CD151 than in its absence. Additionally, several proteins associated with RhoA/ROCK-mediated contractility and trafficking were associated with  $\beta 4$  specifically in the presence or absence of CD151. Importantly, none of the identified proteins were components of HDs, CMSCs or FAs (Fig. 3B; Table S4). These results show that despite the fact that CD151 forms a complex with  $\alpha 6\beta 4$ , this protein does not substantially contribute to the  $\alpha 6\beta 4$  interactome. Furthermore, these findings suggest that the CD151-containing adhesions in the central region of the cells hardly contribute to the interaction between HDs and CMSCs or FAs. Indeed, IF analysis in HaCaT keratinocytes revealed that CMSCs and FAs are assembled in close association with the peripheral HDs, but not the central tetraspanin adhesion structures (Fig. 3C).

In simple epithelial tissues and cell lines, such as intestinal and mammary gland cells, integrin  $\alpha 6\beta 4$  typically resides in type II HDs (Uematsu et al., 1994; Fontao et al., 1997). The group of Aki Manninen used BioID to identify 91 significant cytoplasmic proximity interactors of  $\alpha 6\beta 4$  in Madin Darby Canine kidney

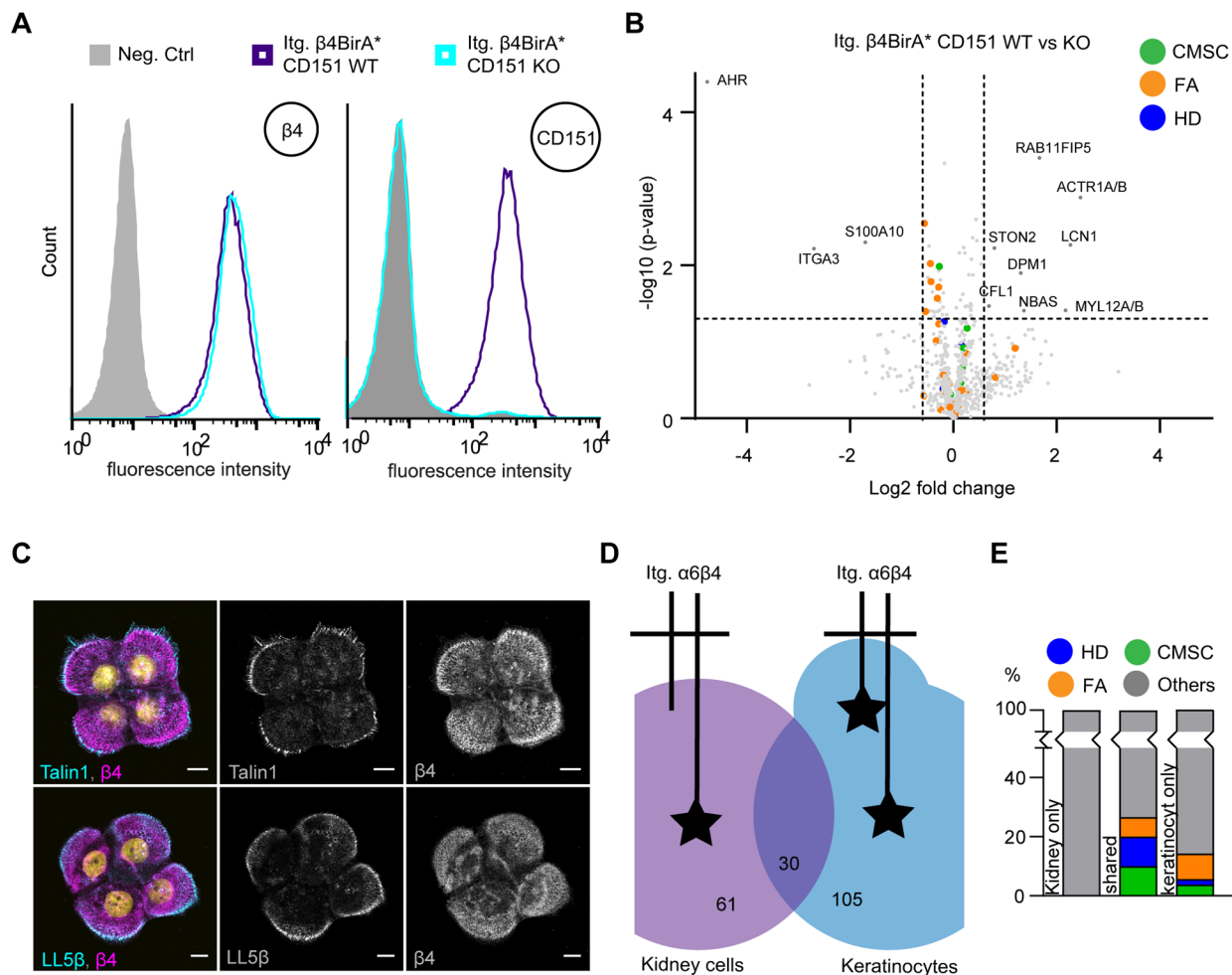


**Fig. 3. CMSC and FA proximity interaction with type I HDs formed at the cells' periphery.** (A) FACS analysis of  $\beta 4$  and CD151 in PA-JEB/ $\beta 4$ -BirA\* CD151 wild-type and CD151 KO cells. (B) Volcano plot showing  $\beta 4$  proximity interactors in the presence and absence of CD151 ( $n=3$ ). (C) Immunofluorescence analysis of wild-type HaCaT keratinocytes showing colocalization of  $\beta 4$  with LL5 $\beta$  and talin1. Scale bars: 10  $\mu$ m. (D) Venn diagram comparing the  $\alpha 6\beta 4$  interactome in keratinocytes with that of  $\beta 4$  in MDCK cells (Myllymäki et al., 2019). Numbers of overlapping and specific proteins are presented. (E) Bar graph showing the percentage of HD, CMSC and FA proteins among the unique interactors of  $\alpha 6\beta 4$  (105) and the  $\beta 4$  (61) in MDCK and PA-JEB/ $\beta 4$  keratinocytes, as well as their percentage among the interactors that are shared between the two interactomes.



epithelial cells (Myllymäki et al., 2019). We compared these interactors with the interactors identified for  $\alpha 6\beta 4$  in keratinocytes and found that only 30 proteins were common between the two data sets (Fig. 3D; Table S5). Although more components of cell matrix complexes were found in keratinocytes than in kidney cells, many of the common hits were CMSC, FA and HD members. These results suggest that the interaction between these complexes is not restricted to type I HDs but also occurs at type II HDs (in kidney cells).

### CMSCs are not required for the formation of HDs and vice versa

Our finding that CMSC proteins are found in close proximity of  $\alpha 6\beta 4$  containing HDs raises the question whether this complex plays a role in the formation of HDs by providing a platform at the plasma membrane for the delivery of exocytotic vesicles carrying specific HD components. To investigate the contribution of CMSCs in the formation of HDs, we generated stable liprin  $\alpha 1$  and  $\beta 1$  knockdown PA-JEB/ $\beta 4$  keratinocytes by short hairpin RNA (shRNA)-mediated RNA interference. Efficient knockdown of these proteins was confirmed by western blot analysis (Fig. 4A,B). Quantification of the protein levels showed that all shRNAs reduced the expression of their targeted proteins by at least 80% (Fig. 4B). Knockdown of liprin  $\alpha 1$  or  $\beta 1$  almost completely prevented the formation of CMSCs as judged by immunofluorescence (Fig. 4C,D). However, HD formation, assessed by  $\beta 4$ -plectin colocalization, was unaffected by the loss of the CMSCs (Fig. 4E).

To investigate if, conversely, HDs affect the formation of the CMSCs, we compared the presence of CMSCs in the presence or absence of HDs by using PA-JEB keratinocytes that express  $\beta 4$  upon doxycycline induction. The expression of  $\beta 4$  was time-dependent and reached a maximum at 24 h after induction (Fig. 5A). Immunofluorescence analysis of  $\beta 4$ -deficient and -proficient cells (assessed after 24 h doxycycline induction) showed no obvious difference in the cellular distribution of CMSC protein localization. Moreover, no difference in the clustering intensities of CMSC proteins were observed (Fig. 5B,C).

In summary, this data show that under steady state conditions the assembly of HDs and CMSCs are not dependent on each other.

### DISCUSSION

In this study, we identified 135 interactors of the integrin  $\alpha 6\beta 4$ , which include amongst others several FA proteins and all components of the CMSC complex. Recent evidence suggests that CMSCs contribute to FA turnover by facilitating integrin  $\beta 1$  recycling and enabling directional transport of MMPs via microtubules (Asperti et al., 2010; Astro et al., 2014; Mana et al., 2016). In a similar way, CMSCs may regulate the turnover of HDs. Indeed, it has been shown that the recycling of  $\alpha 6\beta 4$  is dependent on Arf6, which cooperates with microtubules in adhesion-dependent trafficking (Balasubramanian et al., 2007; Osmani et al., 2018). Furthermore, CMSCs might play a role in the directional transport of HD-associated proteins to sites where new HDs are formed. In agreement with this hypothesis, basal microtubules have been shown to control the integrity of the basement membrane in avian development (Nakaya et al., 2008), and CMSCs are located at substratum adhesion sites composed of deposited laminin-5 and laminin-binding integrins (Hotta et al., 2010). It is perhaps interesting to mention here, that MTs have also been implicated in the assembly of desmosomes, intercellular junctions, which like HDs, are anchored to the intermediate filament system. The adhesion strength of desmosomes is dramatically weakened in the

absence of the MT motor proteins kinesin-1 and kinesin-2, despite the fact that the desmosomal plaque proteins are not affected (Nekrasova et al., 2011).

However, despite these findings and the fact that CMSCs are found in close proximity of type I HDs in the periphery of the cells, as determined by immunofluorescence and BioID, no defects in HD assembly were observed in keratinocytes depleted of liprin  $\alpha 1$  or liprin  $\beta 1$ , which causes the disruption of the CMSC. Likewise, the depletion of LL5 in MCF-10A cells did not affect the basal localization of  $\alpha 6\beta 4$  (Hotta et al., 2010). However, because our investigations involve the analysis of HDs under steady-state conditions, subtle differences in the dynamics and/or the rate of HD maturation may have been unnoticed. Furthermore, it is possible that the loss of CMSC function is compensated for by other proteins that can anchor MTs at the plasma membrane or the actin cortex (Kodama et al., 2003; Wen et al., 2004; Akhmanova and Hoogenraad, 2005; Wickström et al., 2010; Sakamoto et al., 2012; Moffat et al., 2017). These proteins include APC, IQGAP and ACF7 (also known as MACF1), but none of them were identified in the interactome of the integrin  $\alpha 6\beta 4$ .

The localization of CMSCs in the immediate vicinity of type I HDs raises the question of whether these complexes are linked to each other. As far as we are aware, there are no CMSC-associated proteins identified that can link CMSCs directly to HDs. This in contrast to the interaction between CMSCs and FAs, which is mediated by the binding of KANK to talin in FAs (Bouchet et al., 2016). Recently, we showed that in keratinocytes, FAs and HDs are localized in close proximity to each other and that plectin plays a critical role in the mechanical coupling of these two adhesion structures (Wang et al., 2020). Hence, we believe that the localization of CMSC near HDs is due to the interaction of CMSC with the HD-associated FAs.

Comparison of the  $\beta 4$  interactomes in keratinocytes and MDCK cells revealed an overlap of only 30 interactors. CMSC members were present in both interactomes. However, while in the keratinocytes all CMSC members were identified, in the kidney cells only LL5 $\alpha/\beta$  and ERC1 were identified. This relatively small overlap in the two interactomes might be explained by the use of different cell lines and/or the subcellular localization of integrin  $\alpha 6\beta 4$  in type I versus type II HDs (Myllymäki et al., 2019). However, it could also have a technical reason, since it has been shown that proteomes identified by different hands and methods can differ considerably (Horton et al., 2016). The approach employed by us to determine the  $\beta 4$  interactome differed from the one used by Myllymäki et al. (2019) in that they used a myristoylated C-terminally BirA\*-tagged GFP construct as a negative control, while we used an IL2R-BirA\* construct. Furthermore, we expressed the  $\beta 4$ -BirA\* fusion protein in cells that are deficient in  $\beta 4$ , which exclude possible competition between the fusion protein and endogenous  $\beta 4$  for expression at the cell surface because of the pairing of the  $\alpha 6$  subunit with  $\beta 4$ . Importantly, although the two  $\beta 4$  interactomes differ considerably, CMSC, FA and HD proteins were found as interactors of  $\alpha 6\beta 4$  in both datasets, suggesting that the association of CMSCs, FAs and HDs is not unique to keratinocytes. Besides the identification of the CMSC and FA proteins as proximity interactors of integrin  $\alpha 6\beta 4$ , we observed several proteins that link  $\alpha 6\beta 4$  to cell-cell junctions, such as Discs Large Homolog 1 and 5, Afadin and ERBIN. These interactions might occur by a pool of  $\alpha 6\beta 4$  molecules that are not present in HD-like adhesions but are located at the lateral aspects of cells. ERBIN, which associates with p0071 at cell-cell junctions, has previously been shown to also bind the integrin  $\beta 4$  subunit (Favre et al., 2001; Izawa et al., 2002).

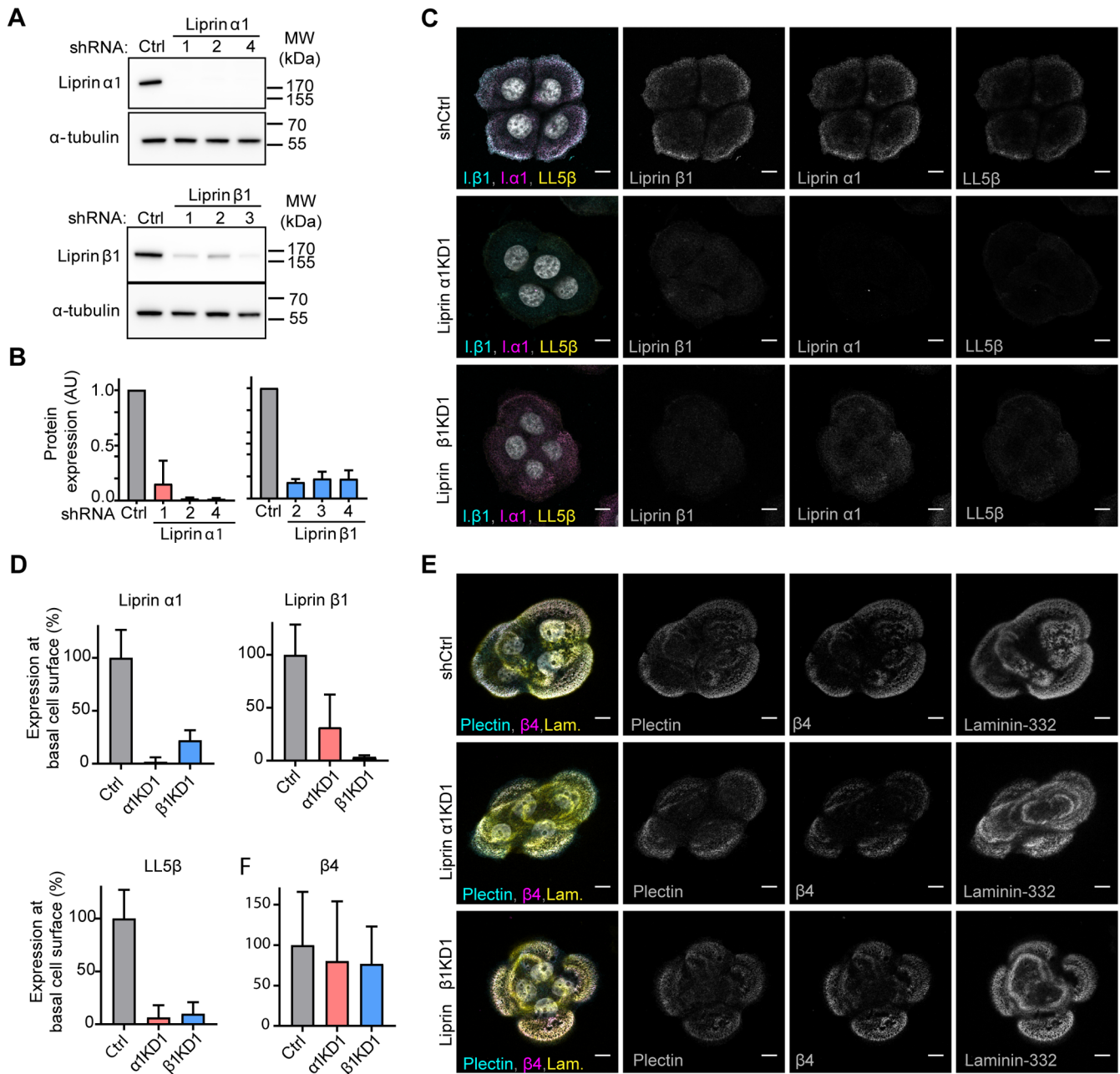


**Fig. 4. CMSCs are not required for the formation of HDs in keratinocytes.** (A) Western blot analysis of stable shRNA-expressing PA-JEB/ $\beta$ 4 cell lines [control (Ctrl) and three knockdowns (KDs)] probed with antibodies against liprin  $\alpha$ 1, liprin  $\beta$ 1 and  $\alpha$ -tubulin. (B) Quantification of liprin protein expression normalized to  $\alpha$ -tubulin protein expression levels in knock down and control PA-JEB/ $\beta$ 4 keratinocytes. Mean+s.d.,  $n=2$ . (C) Triple immunofluorescence detection of liprin  $\alpha$ 1, liprin  $\beta$ 1 and LL5 $\beta$  in liprin  $\alpha$ 1 and  $\beta$ 1 knockdown and control keratinocytes. Scale bars: 10  $\mu$ m. (D) Quantification of immunofluorescence staining of liprin  $\alpha$ 1, liprin  $\beta$ 1 and LL5 $\beta$  in knockdown and control PA-JEB/ $\beta$ 4 keratinocytes ( $n=20$ ). (E) Triple immunofluorescence detection of  $\beta$ 4, plectin and laminin-332 in liprin  $\alpha$ 1 and  $\beta$ 1 knockdown and control PA-JEB/ $\beta$ 4 keratinocytes. Scale bars: 10  $\mu$ m. (F) Quantification of immunofluorescence staining of  $\beta$ 4 shows no significant difference (Mann–Whitney test used) between liprin  $\alpha$ 1 and  $\beta$ 1 knockdown and control PA-JEB/ $\beta$ 4 keratinocytes ( $n=22$ ).

Intriguingly, we also identified the palmitoyl acyltransferase ZDHHC5 as a proximity interactor of the  $\alpha$ 6 and  $\beta$ 4 subunits. Previous studies have shown that in addition to CD151, both  $\alpha$ 6 and  $\beta$ 4 subunits are also palmitoylated (Yang et al., 2004). The enzyme responsible for the palmitoylation of the  $\alpha$ 6 and  $\beta$ 4 subunits in MDA-MB-231 and PC3 cells has been identified as ZDHHC3 (Sharma et al., 2012). Unfortunately, ZDHHC5 has not been tested for its ability to palmitoylate the  $\alpha$ 6 and  $\beta$ 4 subunits; thus, the possibility exists that this enzyme palmitoylates these subunits in a

functional redundant manner. Since palmitoylation stabilizes tetraspanin–tetraspanin interactions as well as their interaction with partner molecules, the palmitoylation of the  $\alpha$ 6 and  $\beta$ 4 subunits may contribute to their stable incorporation into CD151 TEMs that are formed in the central region of the cells.

Although only 11 statistically significant differences were detected between the interactomes of  $\beta$ 4 in the presence and absence of CD151, some of them deserve particular attention because they provide further insights into the role of this tetraspanin

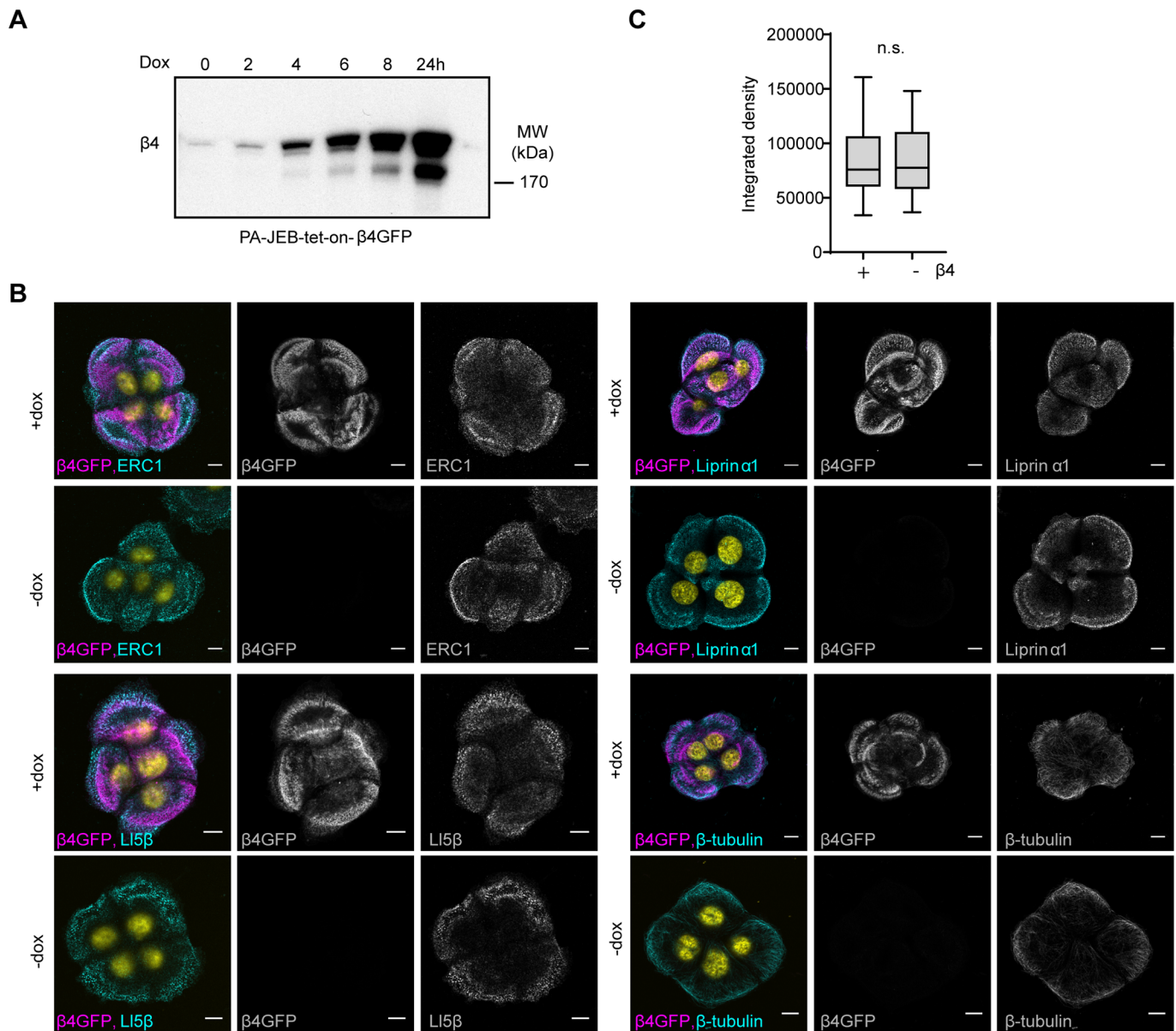


**Fig. 5. HDs are not required for the formation of CMSCs.** (A) Western blot analysis of whole cell lysates from PA-JEB-tet-on-β4-GFP cells treated for different time points with doxycycline, and analyzed for β4. (B) Immunofluorescence analysis of CMSC members in PA-JEB keratinocytes treated with (+) or without (-) doxycycline. Cells were stained for ERC1, liprin α1, LI5β or β-tubulin. Scale bars: 10 μm. (C) Quantification of membrane associated liprin α1, integrated density (area\*intensity), in PA-JEB-tet-on-β4-GFP treated with or without doxycycline for 24 h (n=20). No significant difference; tested with Mann-Whitney test.

in the formation and stabilization of the different α6β4-containing adhesions. For example, the identification of integrin α3β1 as a CD151-dependent interactor of integrin α6β4 supports the recently proposed role of CD151 in the clustering of α3β1, together with α6β4, in central HD-like adhesions (te Molder et al., 2019). Furthermore, the identification of two downstream effectors of the RhoA-ROCK signaling pathway, the myosin regulator light chains 12A/B (MYL12A/B) and cofilin (CFL1), as proximity interactors of β4 in the absence of CD151 is in line with the proposed role of CD151 in regulating RhoA activation (Johnson et al., 2009). Indeed, it has been shown that deletion of CD151 results in elevated RhoA activity (Johnson et al., 2009). CD151 may regulate RhoA activity by preventing α3β1 from becoming incorporated into FAs and thus to support high actomyosin contractility of cells cultured on laminin substrates. The finding that the myosin regulator light chains 12A/B

and cofilin are CD151-dependent proximity interactors of integrin β4 may seem odd at first sight, but can be explained by the increased FA size and the close proximity of these FAs with HDs in the absence of CD151. The ability of CD151 to suppress RhoA activity suggests that CD151 may also contribute to α6β4's ability to counteract cellular tension and traction force in keratinocytes (Wang et al., 2020). Other β4 interactors in the absence of CD151 include several proteins involved in vesicle transport, which suggest that the α6β4 containing adhesions turn over more dynamically in the absence of CD151 than in its presence.

In conclusion, we show that the integrin α6β4 interactome comprises 135 proteins, and includes amongst others FA proteins and components of the CMSC complex, but also many novel proteins that offer opportunities for future research into their role in the assembly of the different α6β4 adhesions.



## MATERIALS AND METHODS

### Reagents

The primary antibodies used in this study are listed in Table 1. Conjugated antibody against biotinylated proteins was streptavidin-HRP (RPN1231 from GE Healthcare). Secondary antibodies for western blot were goat anti-mouse IgG HRP (Bio-Rad; 1:3000) and polyclonal goat anti-rabbit IgG HRP (Dako; 1:5000). Secondary antibody for FACS was donkey anti-mouse IgG PE (Jackson ImmunoResearch; 1:400). Secondary antibodies for IF (1:200) were goat anti-guinea pig IgG Alexa Fluor 488 (A-11073), goat anti-rabbit Alexa Fluor 647 (A-21245), goat anti-rabbit Alexa Fluor 594 (A-21207), goat anti-rat-TxR (T-6392) and goat anti-mouse Alexa Fluor 647 (A-21236) from Invitrogen, goat anti-mouse FITC (Rockland; 610-102-121) and Hamster-Cy5 (Jackson ImmunoResearch; 107-005-142).

### Cell culture

PA-JEB immortalized keratinocytes were isolated from a patient with Pyloric Atresia associated with Junctional Epidermolysis Bullosa. PA-JEB/ $\beta$ 4 keratinocytes stably expressing wild-type  $\beta$ 4 were generated by retroviral transduction (Sterk et al., 2000) and maintained in serum-free keratinocyte medium (KGM; Invitrogen), supplemented with 50  $\mu$ g ml<sup>-1</sup> bovine pituitary gland extract, 5 ng ml<sup>-1</sup> EGF, and antibiotics (100 units ml<sup>-1</sup> streptomycin and 100 units ml<sup>-1</sup> penicillin; Sigma-Aldrich). HaCaT keratinocytes (obtained from the American Type Culture Collection) were cultured in Dulbecco's modified Eagle's medium (DMEM; Gibco) containing 10% heat-inactivated fetal calf serum (FCS; Serana Europe GmbH, Pessin, Germany), and antibiotics. All cells were cultured at 37°C in a humidified, 5% CO<sub>2</sub> atmosphere.

### Cell culture and generation of stable cell lines

Cell lines stably expressing teton- $\beta$ 4-GFP,  $\beta$ 4-BirA\*,  $\alpha$ 6-BirA\* or IL2R-BirA\* were generated by retrovirus-mediated transduction. Virus was produced by transient transfection of Phoenix-ampho cells with retroviral vector constructs using calcium phosphate precipitation and added to the cells. Cells expressing the protein of interest were enriched by puromycin or zeocin selection and bulk sorted by FACS. The tetON- $\beta$ 4-GFP construct was cloned into the EcoRI site of pRetroX-Tight-Puro vector. The  $\beta$ 4-BirA\*,  $\alpha$ 6-BirA\* and the IL2R-BirA\* constructs used were cloned into the SnaBI site or HindIII/XbaI sites of the LZRS-IRES-Zeo vector.

PA-JEB/ $\beta$ 4  $\alpha$ 6KO or CD151KO cells were prepared using CRISPR-Cas9 technology. Target sgRNAs against integrin  $\alpha$ 6 (5'CGGTCGGAGCTG-CCCGCA3') or CD151 (5'-CAGGTTCCGACGCTCCTTGA-3') were cloned in the pX330-U6-Chimeric\_BB-CBh-hSpCas9 (Addgene plasmid #42230, deposited by Feng Zhang). The cells were transiently transfected with this plasmid using lipofectamine<sup>®</sup> 2000 (Invitrogen) in OptiMEM (Gibco), and bulk sorted, for the negative population, using a Moflo Asterios (Beckman Coulter) or FACSaria Fusion (BD Biosciences) cell sorter.

Liprin  $\alpha$ 1 and liprin  $\beta$ 1 were depleted by shRNA-mediated KD in PA-JEB/ $\beta$ 4 cells. Recombinant lentiviruses were produced by transient

co-transfection of HEK293T cells with plasmids encoding the vector and helper functions using lipofectamine 2000. Lentiviruses were added to the cells and infected cells were enriched by puromycin selection for 3 days. The shRNAs targeted: liprin  $\alpha$ 1: (1) 5'-GATGACAAGACAACCATAAA-G-3', (2) 5'-TGAGCCTTCCAAGGTACAAAC-3', (3) 5'-GAGGAGAT-TGAAAGTCGAGTT-3'; Liprin  $\beta$ 1: (1) 5'-CATTGGCTCCCTCAATA-TAA-3', (2) 5'-CCAGAGTGTTCATTTCATAT-3', (3) 5'-GCCAAA-GTGAAGCCAAAGAAA-3' and the empty vector was used as negative control.

### Western blot analysis

Subconfluent cells were washed in cold PBS, lysed in RIPA (1% NP-40, 0.5% sodium deoxycholate, 0.1% SDS, 4 mM EDTA pH 7.5, 100 mM NaCl, 20 mM Tris-HCl pH 7.5) supplemented with 1.5 mM Na<sub>3</sub>VO<sub>4</sub>, 15 mM NaF as phosphatase inhibitors and a protease inhibitor cocktail (1:500; Sigma-Aldrich). Cell lysates were cleared by centrifugation at 12,000 rpm, 1 h at 4°C, supplemented with SDS sample buffer (50 mM Tris-HCl pH 6.8, 2% SDS, 10% glycerol, 12.5 mM EDTA, 0.02% Bromophenol Blue) with  $\beta$ -mercaptoethanol and heated for 5 min at 95°C. Proteins were separated on 4–12% bolt gradient gels (Invitrogen) and transferred to Immobilon-P transfer membranes (Millipore). The membrane was blocked for 3 h in 2% BSA in TBST (10 mM Tris (pH 7.5), 150 mM NaCl, 0.05% Tween 20) before incubation with primary antibody overnight at 4°C and with secondary antibody for 1 h at room temperature or with conjugated Ab for 4 h. After each incubation step, the membranes were washed twice with TBST and twice with TBS (TBST without Tween 20). Antibodies were detected using Clarity Western ECL Substrate (Bio-Rad). Quantification of protein expression was performed on two independent experiments using ImageJ.

### Flow cytometry analysis

Subconfluent cells were trypsinized and collected in PBS supplemented with 2% FCS. Cells were incubated for 50–60 min with primary antibody on ice, washed twice with ice-cold PBS/2% FCS and subsequently incubated with secondary antibody for 50 min on ice. After washing with 2% FCS in PBS, the cells were passed through a nylon mesh filter and 50,000 positive cells were analyzed per sample using a FACSCalibur cell analyzer (BD Biosciences). Unstained cells or cells treated only with secondary antibody were used as negative controls.

### Immunofluorescence

Cells were grown on uncoated coverslips for 20 h before changing the medium to DMEM supplemented with 10% FCS to facilitate HD formation. 20 h after changing the medium the cells were washed with PBS, fixed with 2% PFA for 10 min, permeabilized with 0.2% triton for 5 min and blocked with 2% BSA (Serva) in PBS for 1 h. Cells were incubated with primary and secondary antibodies for 50–60 min each with PBS washing steps in between. Nuclei were stained with DAPI for 20 s and coverslips were

**Table 1. List of primary antibodies, including application, dilution and source**

Target	Antibody	Application	Source
$\alpha$ -tubulin	B-5-1-2; Mouse mAb	WB (1:10,000)	Sigma-Aldrich T5168
$\beta$ -tubulin	Mouse mAb	IF (1:200)	Amersham N357
CD151	5C11; Mouse mAb	FACS (1:1 Sup)	Kind gift from F. Berdichevsky
ERC1	Rabbit pAb	IF (1:500)	Gift from K. Hiroshi
Itg. $\alpha$ 6	GoH3; Rat mAb	IF (1:1 Sup)	Homemade
Itg. $\alpha$ 6	AA6NT; Rabbit pAb	WB (1:500)	Kind gift from A. Cress
Itg. $\beta$ 4	Rabbit pAb	IF (1:1000), WB (1:5000)	Homemade
Itg. $\beta$ 4	439-9B; Rat mAb	IF (1:200)	Kind gift from S. Kennel
Itg. $\beta$ 4	PE-conjugated Rat mAb	FACS (1:400)	BD Pharm. 555720
Laminin-332	R14; Rabbit pAb	IF (1:500)	Kind gift from M. Aumailley
Liprin $\alpha$ 1	Rabbit pAb	IF (1:200), WB (1:1000)	Proteintech 14175-1AP
Liprin $\beta$ 1	Mouse mAb	IF (1:200), WB (1:200)	Santa Cruz Biotechnology 514575
LL5 $\beta$ (PHLDB2)	Hamster mAb	IF (1:200)	Kind gift from J. Sanes
Plectin	P1; Guinea Pig pAb	IF (1:500)	Kind gift from H. Herrmann
Talin1	8D4; Mouse mAb	IF (1:100)	Abcam 157808

mounted on slides using MOWIOL. After drying the slides overnight, cell islands of four cells were imaged using a Leica TCS SP5 confocal microscope with a 63× objective. Quantification of the intensity, integrated density/expression at the basal cell surface in 20–22 islands was performed using ImageJ.

### BioID sample preparation

Cells were seeded for 24 h in biotin-depleted keratinocyte medium before being treated with 50 μM biotin (Sigma-Aldrich #B4501) for 20 h in DMEM/10% FCS. After washing with cold PBS, cells were lysed at 4°C in NP40 lysis buffer (1% Nonidet P-40, 20 mM Tris-HCl, pH 7.5, 100 mM NaCl, and 4 mM EDTA) supplemented with Na<sub>3</sub>VO<sub>4</sub> (1.5 mM), NaF (15 mM) and protease inhibitor cocktail (1:1000; Sigma-Aldrich). Collected whole cell lysates were cleared by centrifugation at 12,000 rpm for 60 min at 4°C and cleared cell lysates were incubated with Streptavidin Sepharose High Performance beads (GE Healthcare) overnight at 4°C. After incubation beads were washed with NP40 lysis buffer, cold PBS and beads were stored at –80°C.

### Mass spectrometry analysis

Peptide mixtures were prepared from three replicate experiments, measured and analyzed as previously described (Wang et al., 2020), with the following exceptions. The MS/MS data were searched against the human SwissProt database (20,367 entries, release 2020\_01) complemented with a list of common contaminants and concatenated with the reversed version of all sequences. Differentially expressed proteins were determined using a Student's *t*-test (minimum threshold  $P \leq 0.05$  and  $[x/y] \geq 0.6$  and  $[x/y] \leq -0.6$ ).

### Acknowledgements

We thank all colleagues for kindly providing reagents and constructs, and Alba Zuidema, Veronika Ramovs and Kevin Wilhelmsen for critical reading of the manuscript.

### Competing interests

The authors declare no competing or financial interests.

### Author contributions

Conceptualization: L.t.M., A.S.; Methodology: L.t.M., L.H.; Validation: L.t.M., O.B.; Investigation: L.t.M., L.H., M.K.; Data curation: L.t.M., A.S.; Writing - original draft: L.t.M.; Writing - review & editing: A.S.; Supervision: O.B., A.S.; Funding acquisition: A.S.

### Funding

This work was supported by grants from the Netherlands Organization for Scientific Research (NWO; project number 824.14.010) and the Dutch Cancer Society (project number 2013-5971).

### Data availability

The data that support the findings of this study are available upon reasonable request from the corresponding author (A.S.).

### Supplementary information

Supplementary information available online at <https://bio.biologists.org/lookup/doi/10.1242/bio.054155.supplemental>

### References

- Akhmanova, A. and Hoogenraad, C. C.** (2005). Microtubule plus-end-tracking proteins: mechanisms and functions. *Curr. Opin. Cell Biol.* **17**, 47–54. doi:10.1016/j.ccb.2004.11.001
- Akhmanova, A. and Steinmetz, M. O.** (2008). Tracking the ends: a dynamic protein network controls the fate of microtubule tips. *Nat. Rev. Mol. Cell Biol.* **9**, 309–322. doi:10.1038/nrm2369
- Akhmanova, A., Stehbens, S. J. and Yap, A. S.** (2009). Touch, grasp, deliver and control: functional cross-talk between microtubules and cell adhesions. *Traffic* **10**, 268–274. doi:10.1111/j.1600-0854.2008.00869.x
- Asperti, C., Pettinato, E. and de Curtis, I.** (2010). Liprin-α1 affects the distribution of low-affinity β1 integrins and stabilizes their permanence at the cell surface. *Exp. Cell Res.* **316**, 915–926. doi:10.1016/j.yexcr.2010.01.017
- Astro, V., Chiaretti, S., Magistrati, E., Fivaz, M. and de Curtis, I.** (2014). Liprin-α1, ERC1 and LL5 define polarized and dynamic structures that are implicated in cell migration. *J. Cell Sci.*, **127**, 3862–3876. doi:10.1242/jcs.155663
- Balasubramanian, N., Scott, D. W., Castle, J. D., Casanova, J. E. and Schwartz, M. A.** (2007). Arf6 and microtubules in adhesion-dependent trafficking of lipid rafts. *Nat. Cell Biol.* **9**, 1381–1391. doi:10.1038/ncb1657
- Blanchoin, L., Boujemaa-Paterski, R., Sykes, C. and Plastino, J.** (2014). Actin dynamics, architecture, and mechanics in cell motility. *Phys. Rev.* **94**, 235–263. doi:10.1152/physrev.00018.2013
- Bouchet, B. P., Gough, R. E., Ammon, Y.-C., van de Willige, D., Post, H., Jacquemet, G., Altelaar, A. F. M., Heck, A. J. R., Goult, B. T. and Akhmanova, A.** (2016). Talin-KANK1 interaction controls the recruitment of cortical microtubule stabilizing complexes to focal adhesions. *eLife* **5**, e18124. doi:10.7554/eLife.18124
- Dogterom, M. and Koenderink, G. H.** (2019). Actin-microtubule crosstalk in cell biology. *Nat. Rev. Mol. Cell Biol.* **20**, 38–54. doi:10.1038/s41580-018-0067-1
- Dong, J.-M., Tay, F. P.-L., Swa, H. L.-F., Gunaratne, J., Leung, T., Burke, B. and Manser, E.** (2016). Proximity biotinylation provides insight into the molecular composition of focal adhesions at the nanometer scale. *Sci. Signal.* **9**, rs4. doi:10.1126/scisignal.aaf3572
- Favre, B., Fontao, L., Koster, J., Shafaatian, R., Jaunin, F., Saurat, J.-H., Sonnenberg, A. and Borradori, L.** (2001). The hemidesmosomal protein bullous pemphigoid antigen 1 and the integrin β4 subunit bind to ERBIN. Molecular cloning of multiple alternative splice variants of ERBIN and analysis of their tissue expression. *J. Biol. Chem.* **276**, 32427–32436. doi:10.1074/jbc.M011005200
- Fontao, L., Dirrig, S., Owaribe, K., Keding, M. and Launay, J. F.** (1997). Polarized expression of HD1: relationship with the cytoskeleton in cultured human colonic carcinoma cells. *Exp. Cell Res.* **231**, 319–327. doi:10.1006/excr.1996.3465
- Fredriksson, K., Van Itallie, C. M., Aponte, A., Gucek, M., Tietgens, A. J. and Anderson, J. M.** (2015). Proteomic analysis of proteins surrounding occludin and claudin-4 reveals their proximity to signaling and trafficking networks. *PLoS ONE* **10**, e0117074. doi:10.1371/journal.pone.0117074
- Has, C. and Bruckner-Tuderman, L.** (2014). The genetics of skin fragility. *Annu. Rev. Genomics Hum. Genet.* **15**, 245–268. doi:10.1146/annurev-genom-090413-025540
- Horton, E. R., Byron, A., Askari, J. A., Ng, D. H. J., Millon-Frémillon, A., Robertson, J., Koper, E. J., Paul, N. R., Warwood, S., Knight, D. et al.** (2015). Definition of a consensus integrin adhesome and its dynamics during adhesion complex assembly and disassembly. *Nat. Cell Biol.* **17**, 1577–1587. doi:10.1038/ncb3257
- Horton, E. R., Humphries, J. D., James, J., Jones, M. C., Askari, J. A. and Humphries, M. J.** (2016). The integrin adhesome network at a glance. *J. Cell Sci.* **129**, 4159–4163. doi:10.1242/jcs.192054
- Hotta, A., Kawakatsu, T., Nakatani, T., Sato, T., Matsui, C., Sukezane, T., Akagi, T., Hamaji, T., Grigoriev, I., Akhmanova, A. et al.** (2010). Laminin-based cell adhesion anchors microtubule plus ends to the epithelial cell basal cortex through LL5α/β. *J. Cell Biol.* **189**, 901–917. doi:10.1083/jcb.200910095
- Izawa, I., Nishizawa, M., Tomono, Y., Ohtakara, K., Takahashi, T. and Inagaki, M.** (2002). ERBIN associates with p0071, an armadillo protein, at cell-cell junctions of epithelial cells. *Genes Cells* **7**, 475–485. doi:10.1046/j.1365-2443.2002.00533.x
- Johnson, J. L., Winterwood, N., DeMali, K. A. and Stipp, C. S.** (2009). Tetraspanin CD151 regulates RhoA activation and the dynamic stability of carcinoma cell-cell contacts. *J. Cell Sci.* **122**, 2263–2273. doi:10.1242/jcs.045997
- Kirfel, J., Magin, T. M. and Reichelt, J.** (2003). Keratins: a structural scaffold with emerging functions. *Cell. Mol. Life Sci.* **60**, 56–71. doi:10.1007/s000180300004
- Kodama, A., Karakesisoglou, I., Wong, E., Vaezi, A. and Fuchs, E.** (2003). ACF7: an essential integrator of microtubule dynamics. *Cell* **115**, 343–354. doi:10.1016/S0092-8674(03)00813-4
- Lansbergen, G., Grigoriev, I., Mimori-Kiyosue, Y., Ohtsuka, T., Higa, S., Kitajima, I., Demmers, J., Galjart, N., Houtsmuller, A. B., Grosveld, F. et al.** (2006). CLASPs attach microtubule plus ends to the cell cortex through a complex with LL5β. *Dev. Cell* **11**, 21–32. doi:10.1016/j.devcel.2006.05.012
- Litjens, S. H. M., de Pereda, J. M. and Sonnenberg, A.** (2006). Current insights into the formation and breakdown of hemidesmosomes. *Trends Cell Biol.* **16**, 376–383. doi:10.1016/j.tcb.2006.05.004
- Mana, G., Clapero, F., Panieri, E., Panero, V., Böttcher, R. T., Tseng, H.-Y., Saltarin, F., Astanina, E., Wolanska, K. I., Morgan, M. R. et al.** (2016). PPF1A1 drives active α5β1 integrin recycling and controls fibronectin fibrillogenesis and vascular morphogenesis. *Nat. Commun.* **7**, 13546. doi:10.1038/ncomms13546
- Mimori-Kiyosue, Y., Grigoriev, I., Lansbergen, G., Sasaki, H., Matsui, C., Severin, F., Galjart, N., Grosveld, F., Vorobjev, I., Tsukita, S. et al.** (2005). CLASP1 and CLASP2 bind to EB1 and regulate microtubule plus-end dynamics at the cell cortex. *J. Cell Biol.* **168**, 141–153. doi:10.1083/jcb.200405094
- Moffat, J. J., Ka, M., Jung, E.-M., Smith, A. L. and Kim, W.-Y.** (2017). The role of MACF1 in nervous system development and maintenance. *Semin. Cell Dev. Biol.* **69**, 9–17. doi:10.1016/j.semdb.2017.05.020
- Myllymäki, S.-M., Kämäräinen, U.-R., Liu, X., Cruz, S. P., Miettinen, S., Vuorela, M., Varjosalo, M. and Manninen, A.** (2019). Assembly of the β4-Integrin Interactome Based on Proximal Biotinylation in the Presence and Absence of Heterodimerization. *Mol. Cell. Proteomics* **18**, 277–293. doi:10.1074/mcp.RA118.001095
- Nakaya, Y., Sukowati, E. W., Wu, Y. and Sheng, G.** (2008). RhoA and microtubule dynamics control cell-basement membrane interaction in EMT during gastrulation. *Nat. Cell Biol.* **10**, 765–775. doi:10.1038/ncb1739

- Nekrasova, O. E., Amargo, E. V., Smith, W. O., Chen, J., Kreitzer, G. E. and Green, K. J.** (2011). Desmosomal cadherins utilize distinct kinesins for assembly into desmosomes. *J. Cell Biol.* **195**, 1185-1203. doi:10.1083/jcb.201106057
- Osmani, N., Pontabry, J., Comelles, J., Fekonja, N., Goetz, J. G., Riveline, D., Georges-Labouesse, E. and Labouesse, M.** (2018). An Arf6- and caveolae-dependent pathway links hemidesmosome remodeling and mechanoresponse. *Mol. Biol. Cell* **29**, 435-451. doi:10.1091/mbc.E17-06-0356
- Ramovs, V., te Molder, L. and Sonnenberg, A.** (2017). The opposing roles of laminin-binding integrins in cancer. *Matrix Biol.* **57-58**, 213-243. doi:10.1016/j.matbio.2016.08.007
- Rodriguez, O. C., Schaefer, A. W., Mandato, C. A., Forscher, P., Bement, W. M. and Waterman-Storer, C. M.** (2003). Conserved microtubule-actin interactions in cell movement and morphogenesis. *Nat. Cell Biol.* **5**, 599-609. doi:10.1038/ncb0703-599
- Roux, K. J., Kim, D. I., Raida, M. and Burke, B.** (2012). A promiscuous biotin ligase fusion protein identifies proximal and interacting proteins in mammalian cells. *J. Cell Biol.* **196**, 801-810. doi:10.1083/jcb.201112098
- Sakamoto, S., Ishizaki, T., Okawa, K., Watanabe, S., Arakawa, T., Watanabe, N. and Narumiya, S.** (2012). Liprin- $\alpha$  controls stress fiber formation by binding to mDia and regulating its membrane localization. *J. Cell Sci.* **125**, 108-120. doi:10.1242/jcs.087411
- Sharma, C., Rabinovitz, I. and Hemler, M. E.** (2012). Palmitoylation by DHHC3 is critical for the function, expression, and stability of integrin  $\alpha 6 \beta 4$ . *Cell. Mol. Life Sci.* **69**, 2233-2244. doi:10.1007/s00018-012-0924-6
- Sonnenberg, A., Calafat, J., Janssen, H., Daams, H., van der Raaij-Helmer, L. M. H., Falcioni, R., Kennel, S. J., Aplin, J. D., Baker, J., Loizidou, M. et al.** (1991). Integrin  $\alpha 6 / \beta 4$  complex is located in hemidesmosomes, suggesting a major role in epidermal cell-basement membrane adhesion. *J. Cell Biol.* **113**, 907-917. doi:10.1083/jcb.113.4.907
- Stehbens, S. J., Paszek, M., Pemble, H., Ettinger, A., Gierke, S. and Wittmann, T.** (2014). CLASPs link focal-adhesion-associated microtubule capture to localized exocytosis and adhesion site turnover. *Nat. Cell Biol.* **16**, 558-570. doi:10.1038/ncb2975
- Sterk, L. M. T., Geuijen, C. A. W., Oomen, L. C., Calafat, J., Janssen, H. and Sonnenberg, A.** (2000). The tetraspan molecule CD151, a novel constituent of hemidesmosomes, associates with the integrin  $\alpha 6 \beta 4$  and may regulate the spatial organization of hemidesmosomes. *J. Cell Biol.* **149**, 969-982. doi:10.1083/jcb.149.4.969
- te Molder, L., Juksar, J., Harkes, R., Wang, W., Kreft, M. and Sonnenberg, A.** (2019). Tetraspanin CD151 and integrin  $\alpha 3 \beta 1$  contribute to the stabilization of integrin  $\alpha 6 \beta 4$ -containing cell-matrix adhesions. *J. Cell Sci.* **132**, jcs.235366. doi:10.1242/jcs.235366
- Uematsu, J., Nishizawa, Y., Sonnenberg, A. and Owaribe, K.** (1994). Demonstration of type II hemidesmosomes in a mammary gland epithelial cell line, BMGE-H1. *J. Biochem.* **115**, 469-476. doi:10.1093/oxfordjournals.jbchem.a124361
- van Itallie, C. M., Aponte, A., Tietgens, A. J., Gucsek, M., Fredriksson, K. and Anderson, J. M.** (2013). The N and C termini of ZO-1 are surrounded by distinct proteins and functional protein networks. *J. Biol. Chem.* **288**, 13775-13788. doi:10.1074/jbc.M113.466193
- van Itallie, C. M., Tietgens, A. J., Aponte, A., Fredriksson, K., Fanning, A. S., Gucsek, M. and Anderson, J. M.** (2014). Biotin ligase tagging identifies proteins proximal to E-cadherin, including lipoma preferred partner, a regulator of epithelial cell-cell and cell-substrate adhesion. *J. Cell Sci.* **127**, 885-895. doi:10.1242/jcs.140475
- Walko, G., Castañón, M. J. and Wiche, G.** (2015). Molecular architecture and function of the hemidesmosome. *Cell Tissue Res.* **360**, 529-544. doi:10.1007/s00441-015-2216-6
- Wang, W., Zuidema, A., Te Molder, L., Nahidiazar, L., Hoekman, L., Schmidt, T., Coppola, S. and Sonnenberg, A.** (2020). Hemidesmosomes modulate force generation via focal adhesions. *J. Cell Biol.* **219**, 1-19. doi:10.1083/jcb.201904137
- Wen, Y., Eng, C. H., Schmoranzler, J., Cabrera-Poch, N., Morris, E. J. S., Chen, M., Wallar, B. J., Alberts, A. S. and Gundersen, G. G.** (2004). EB1 and APC bind to mDia to stabilize microtubules downstream of Rho and promote cell migration. *Nat. Cell Biol.* **6**, 820-830. doi:10.1038/ncb1160
- Wickström, S. A., Lange, A., Hess, M. W., Polleux, J., Spatz, J. P., Krüger, M., Pfaller, K., Lambacher, A., Bloch, W., Mann, M. et al.** (2010). Integrin-linked kinase controls microtubule dynamics required for plasma membrane targeting of caveolae. *Dev. Cell* **19**, 574-588. doi:10.1016/j.devcel.2010.09.007
- Yang, X., Kovalenko, O. V., Tang, W., Claas, C., Stipp, C. S. and Hemler, M. E.** (2004). Palmitoylation supports assembly and function of integrin-tetraspanin complexes. *J. Cell Biol.* **167**, 1231-1240. doi:10.1083/jcb.200404100